Cambridge International
Science Publishing
Cambridge CB1 6AZ
Great Britain

Journal of Computational Methods in Sciences and Engineering
vol. 2, no. 1-2, 2002, pp. 125–134
ISSN 1472–7978

Free-Energy Barriers in Spin Glasses from Multi-Overlap Simulations[1]

Wolfhard Janke[2]

Institut für Theoretische Physik, Universität Leipzig,
04109 Leipzig, Germany.
E-mail: wolfhard.janke@itp.uni-leipzig.de

Bernd A. Berg

Department of Physics, The Florida State University, Tallahassee, FL 32306, USA.
E-mail: berg@mailer.csit.fsu.edu

Alain Billoire

CEA/Saclay, Service de Physique Théorique, 91191 Gif-sur-Yvette, France.
E-mail: billoir@spht.saclay.cea.fr

Received 30 April, 2001; accepted in revised form 30 July, 2001

Abstract: We present results of recent high statistics Monte Carlo studies of the Edwards-Anderson Ising spin-glass model in three and four dimensions. The simulations are based on a non-Boltzmann sampling technique, the multi-overlap algorithm which will be briefly reviewed. Physically we mainly discuss those properties of the probability density $P_{\mathcal{J}}(q)$ of the Parisi overlap parameter q which are difficult to obtain with standard canonical Boltzmann sampling. In particular we focus on the free-energy barriers F_B^q which are visible in $P_{\mathcal{J}}(q)$ and the behavior of the tails of the averaged probability density.

Keywords: Spin glasses; Monte Carlo simulations; multi-overlap algorithm; free-energy barriers.

PACS: 75.10.Nr Spin-glass and other random models; 75.40.Mg Numerical simulation studies; 75.50.Lk Spin glasses and other random magnets.

1 Introduction

For more than twenty years, the peculiar behavior of the low-temperature phase of spin glasses [1, 2, 3, 4] has attracted the interest of many workers employing a variety of different approaches. Despite the large amount of experimental, mathematical, theoretical and simulational work done, the physical mechanisms underlying these phenomena are not yet fully understood. To cope with the enormous complexity of the problem, various levels of simplified models have been studied theoretically. The mean-field approximation [5] is expected to become accurate in high dimensions,

[1]Work partially supported by the German-Israel-Foundation (GIF-I-0438-145.07/95), the US Department of Energy (DOE-DE-FG02-97ER41022), and by the T3E computer-time grants p526 (CEA, Grenoble), bvpl01 (ZIB, Berlin), and hmz091 (NIC, Jülich).

[2]The address for manuscript correspondence: Wolfhard Janke, Institut für Theoretische Physik, Universität Leipzig, Augustusplatz 10/11, 04109 Leipzig, Germany. Phone: +49 341 9732 725. Fax: +49 341 9732 747. E-mail: wolfhard.janke@itp.uni-leipzig.de

but its status is unclear in physical dimensions, where an alternative droplet approximation [6] has been proposed. The two treatments yield conflicting predictions which has prompted quite a controversial discussion over many years. Numerical approaches such as Monte Carlo simulations can, in principle, provide arbitrarily precise results in physical dimensions. In practice, however, the simulational approach is severely hampered by an extremely slow (pseudo-) dynamics of the stochastic process and, as a consequence, the numerical attempts to decide between the two alternatives remained inconclusive.

The origin of the severe slowing down can be traced back to the existence of free-energy barriers separating metastable configurations. Experimentally this is reflected by the phenomenon of aging which is the typical signature of measurements of the remanent magnetization in the spin-glass phase below the freezing point. This characteristic feature can be explained by frustration in the spin configurations which is caused by competing interactions between the magnetic moments. Typical examples for such materials are dilute solutions of transition metal magnetic impurities in noble hosts [1] such as, for instance, Cu-0.9% Mn and $(Fe_{0.15}Ni_{0.85})_{75}P_{16}B_6Al_3$ [7, 8], where randomly distributed impurities induce a magnetic polarization of the host metal electrons being positive at some distances and negative at others.

To overcome the slowing-down problem, various novel simulation techniques have been devised in the past few years. While some of them only aim at improving the (pseudo-) dynamics of the Monte Carlo process, others are in addition also well suited for a quantitative characterization of the free-energy barriers responsible for the slowing-down problem. Among the latter is the multi-overlap algorithm [9] which was recently employed in quite extensive simulations [10, 11] of the Edwards-Anderson [12] Ising spin-glass model in three and four dimensions. The purpose of this note is to describe this algorithm and to summarize our main results obtained with this method.

2 The Model and Simulation Methods

The Edwards-Anderson Ising (EAI) spin-glass model is defined through the energy

$$E = -\sum_{\langle ik \rangle} J_{ik}\, s_i s_k \ , \tag{1}$$

where the sum is over nearest-neighbor pairs of a d-dimensional (hyper-) cubic lattice of size $N = L^d$ with periodic boundary conditions, and the fluctuating spins s_i as well as the quenched exchange coupling constants J_{ik} take on the values ± 1, with equal probabilities. As order parameter one usually takes the Parisi overlap parameter [5]

$$q = \frac{1}{N} \sum_{i=1}^{N} s_i^{(1)}\, s_i^{(2)} \ , \tag{2}$$

where the spin superscripts label two independent (real) replicas for the same realization of randomly chosen exchange coupling constants $\mathcal{J} = \{J_{ik}\}$. For given $\mathcal{J}$ the probability density of q is denoted by $P_{\mathcal{J}}(q)$ and Parisi's function $x_{\mathcal{J}}(q) = \int_{-q}^{q} dq' P_{\mathcal{J}}(q')$ is essentially its cumulative distribution function as, for instance, defined in Ref. [13]. Averages over the quenched disorder are denoted by

$$P(q) = [P_{\mathcal{J}}(q)]_{\rm av} = \frac{1}{\#J} \sum_{\mathcal{J}} P_{\mathcal{J}}(q) \ ; \quad x(q) = [x_{\mathcal{J}}(q)]_{\rm av} = \frac{1}{\#J} \sum_{\mathcal{J}} x_{\mathcal{J}}(q) \ , \tag{3}$$

where $\#J$ $(\to \infty)$ is the number of realizations considered. Below the freezing temperature, in the infinite-volume limit $N \to \infty$, an increasing *continuous* part of $x(q)$ characterizes the mean-field picture [5] of spin glasses, whereas in ferromagnets as well as in the droplet picture [6] of spin glasses $x(q)$ is a step function. Most studies have so far focused on the averaged quantities.

As far as free-energy barriers are concerned, the distribution functions for *individual* realizations $\mathcal{J}$ play the central role. Since it is virtually impossible to get complete control over the full distribution function one has to concentrate on a few characteristic properties. In this work, we concentrated on those free-energy barriers F_B^q which are reflected by the minima of $P_{\mathcal{J}}(q)$. Conventional, canonical Monte Carlo (MC) simulations are not suited for such a study because the likelihood to generate the corresponding configurations in the Gibbs canonical ensemble is very small. This problem is overcome by non-Boltzmann sampling [14, 15] with the multi-overlap weight [9]

$$w_{\mathcal{J}}(q) = \exp\left[-\beta(E_{\mathcal{J}}^{(1)} + E_{\mathcal{J}}^{(2)}) + S_{\mathcal{J}}(q)\right] \ , \tag{4}$$

where $\beta = 1/T$ is the inverse temperature in natural units. $E_{\mathcal{J}}^{(1)}$ and $E_{\mathcal{J}}^{(2)}$ are the energies of the two replicas, coupled by $S_{\mathcal{J}}(q)$ in such a way that a broad histogram in q over the entire accessible range $-1 \le q \le 1$ is obtained. The iterative construction of the weight function $W_{\mathcal{J}}(q) \equiv \exp(S_{\mathcal{J}}(q))$ is the first step of the algorithm. Ideally $W_{\mathcal{J}}$ should satisfy $P_{\mathcal{J}}^{\mathrm{muq}}(q) = P_{\mathcal{J}}(q)W_{\mathcal{J}}(q) = \mathrm{const.}$, i.e., should give rise to a completely flat multi-overlap probability density $P_{\mathcal{J}}^{\mathrm{muq}}(q)$. Since, of course, $P_{\mathcal{J}}(q)$ is a priori unknown, we have to proceed by iteration. Let us thus assume some approximate $W_{\mathcal{J},n}$ is known. The simulation would then yield $P_{\mathcal{J},n}^{\mathrm{muq}}$ which in general is not yet perfectly flat. If $P_{\mathcal{J},n}^{\mathrm{muq}}$ was sampled with arbitrary precision, the desired weight function would be $W_{\mathcal{J}} \propto W_{\mathcal{J},n}/P_{\mathcal{J},n}^{\mathrm{muq}}$. For the update procedure, we are actually only interested in relative transition amplitudes and it is therefore useful to rephrase the iteration in terms of

$$R_{\mathcal{J}}(q) \equiv W_{\mathcal{J}}(q+\Delta q)/W_{\mathcal{J}}(q) = R_{\mathcal{J},n}(q)P_{\mathcal{J},n}^{\mathrm{muq}}(q)/P_{\mathcal{J},n}^{\mathrm{muq}}(q+\Delta q), \tag{5}$$

where $\Delta q = 2/N$ is the step-width in q as defined in Eq (2). When updating the spins in the n*th* iteration, $R_{\mathcal{J},n}(q) = W_{\mathcal{J},n}(q+\Delta q)/W_{\mathcal{J},n}(q)$ has to be considered as a given, fixed function of q. The multi-overlap histogram $P_{\mathcal{J},n}^{\mathrm{muq}}(q)$, however, can never be exactly determined in actual simulations, but is always a noisy estimator whose statistical errors can be estimated by $\sqrt{P_{\mathcal{J},n}^{\mathrm{muq}}(q)}$ (neglecting auto- and cross-correlations and assuming in this section unnormalized histograms counting the number of hits). By taking the logarithm in Eq (5) it is then straightforward to obtain the squared error on $\ln R_{\mathcal{J}}(q)$,

$$\epsilon^2_{\ln R_{\mathcal{J}}(q)} \equiv 1/p(q) = 1/P_{\mathcal{J},n}^{\mathrm{muq}}(q) + 1/P_{\mathcal{J},n}^{\mathrm{muq}}(q+\Delta q). \tag{6}$$

We now have two noisy estimators, $R_{\mathcal{J}}(q)$ and $R_{\mathcal{J},n}(q)$ (with squared inverse errors $p(q)$ and $p_n(q)$), which may be linearly combined to yield an optimized estimator $\ln R_{\mathcal{J},n+1}(q) = \kappa_n(q)\ln R_{\mathcal{J}}(q) + (1-\kappa_n(q))\ln R_{\mathcal{J},n}(q)$, with

$$\kappa_n(q) = p(q)/(p(q)+p_n(q)), \tag{7}$$

such that its statistical error is minimized. By exponentiating the optimized estimator and using Eq (5), we finally arrive at the recursion

$$\begin{aligned} R_{\mathcal{J},n+1}(q) &= R_{\mathcal{J}}(q)^{\kappa_n(q)} R_{\mathcal{J},n}(q)^{1-\kappa_n(q)} \\ &= R_{\mathcal{J},n}(q)\left(P_{\mathcal{J},n}^{\mathrm{muq}}(q)/P_{\mathcal{J},n}^{\mathrm{muq}}(q+\Delta q)\right)^{\kappa_n(q)}, \qquad (8) \\ p_{n+1}(q) &= p(q) + p_n(q). \qquad (9) \end{aligned}$$

Once $W_{\mathcal{J}}(q) = \exp(S_{\mathcal{J}}(q))$ is determined and kept fixed, the system is equilibrated and then the data production is performed. Finally any canonical quantity can be computed by reweighting.

	$3d$, $\beta_0 = 1.0$				$4d$, $\beta_0 = 0.6$			
L	$\#\mathcal{J}$	n_{flip}	n	n_{sw}	$\#\mathcal{J}$	n_{flip}	n	n_{sw}
4	8 192	10	1	0.2×10^6	4 096	10	2	0.4×10^6
6	8 192	10	4	1.0×10^6	4 096	20	8	3.7×10^6
8	8 192	10	16	7.6×10^6	1 024	20-30	16	49.3×10^6
12	640	20	32	154.0×10^6				

Table 1: Number of realizations $\#\mathcal{J}$, number of requested flips n_{flip} during weight construction, number of equilibration sweeps $n \times 65536$, and average number of sweeps per realization n_{sw}.

As a measure for the (pseudo-) dynamics of the multi-overlap algorithm we define an autocorrelation time $\tau_{\mathcal{J}}^{\text{muq}}$ by counting the average number of sweeps it takes to evolve the overlap parameter from $q = 0 \to q = \pm 1$ and back. Recalling the dynamics of first-order phase transitions, we shall adopt the usual terminology and call such a cycle a "tunneling" event. The iteration for the weight construction was stopped after n_{flip} "tunneling" events occurred, cf. Table 1. Each production run of data taking was concluded after at least 20 "tunneling" events. To allow for standard reweighting in temperature, we stored not only $P_{\mathcal{J}}(q)$ but also the time series of measurements of the order parameter, the energies and the magnetizations of the two replicas. The number of sweeps between measurements was adjusted by an adaptive data compression routine to ensure that each time series consists of $2^{16} = 65536$ measurements separated by approximately $\tau_{\mathcal{J}}^{\text{muq}}$ sweeps.

3 Results

Here we shall concentrate only on the simulations in the spin-glass phase. The simulation points are $\beta_0 = 1.0 > \beta_c = 0.90 \pm 0.03$ (Ref. [16]) in three dimensions ($3d$) and $\beta_0 = 0.6 > \beta_c = 0.485 \pm 0.005$ (Ref. [17]) in four dimensions ($4d$). The Table 1 gives an overview of the number of simulated realizations, $\#\mathcal{J}$, and the average length of the runs, n_{sw}. The J_{ik} realizations were drawn using the pseudo random number generators RANMAR [18] and RANLUX [19] (luxury level 4). In the simulations themselves we always employed the faster RANMAR generator.

3.1 Autocorrelation Times of the Multi-Overlap Algorithm

For each realization we measured the autocorrelation time $\tau_{\mathcal{J}}^{\text{muq}}$. Fitting the averages over the realizations $\mathcal{J}$ to the power-law ansatz $\ln([\tau_{\mathcal{J}}^{\text{muq}}]_{\text{av}}) = a + z\,\ln(N)$ we obtained $z = 2.32 \pm 0.07$ in $3d$ and $z = 1.94 \pm 0.02$ in $4d$. The quality of the fits is bad; see Figure 1 where for comparison also exponential fits are shown. But they clearly show that the slowing down is quite off from the theoretical optimum $z = 1$ one would expect if the free-energy barriers visible in the overlap parameter q were the only cause for the slowing down of the canonical dynamics. In this case, the multi-overlap autocorrelation time $\tau_{\mathcal{J}}^{\text{muq}}$ should be dominated by a random walk behavior between $q = -1$ and $q = +1$ and scale proportional to N in units of sweeps in the limit of perfect flattening. In multicanonical simulations (with broad energy histograms) of the $3d$ model an even larger exponent $z = 2.8 \pm 0.1$ has been observed [20]. The large values of z imply that the canonical overlap barriers cannot be the exclusive cause for the slowing down of spin-glass dynamics below the freezing point, i.e., the projection of the multi-dimensional phase space onto the q direction hides important features of the free-energy landscape of the model.

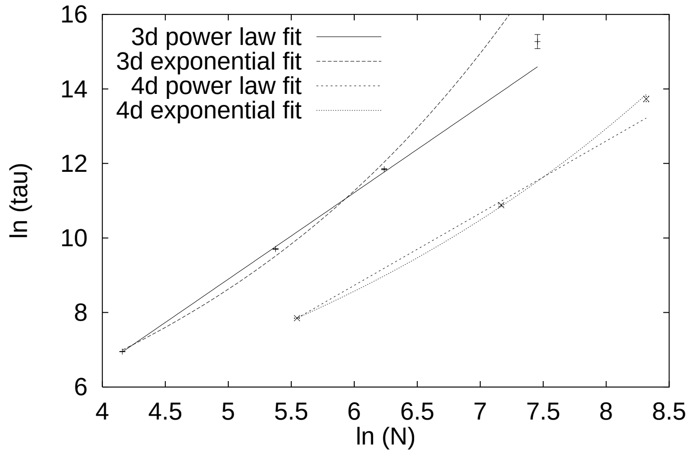

Figure 1: Average autocorrelation times $[\tau_{\mathcal{J}}^{\rm muq}]_{\rm av}$ of the multi-overlap algorithm.

3.2 Finite-Size Scaling Behavior of Free-Energy Barriers

Our effective free-energy barriers F_B^q are defined through an auxiliary $1d$ Metropolis-Markov chain [21] which has the canonical $P_{\mathcal{J}}(q)$ probability density as its equilibrium distribution. The tridiagonal transition matrix

$$T = \begin{bmatrix} 1-w_{2,1} & w_{1,2} & 0 & \dots \\ w_{2,1} & 1-w_{1,2}-w_{3,2} & w_{2,3} & \dots \\ 0 & w_{3,2} & 1-w_{2,3}-w_{4,3} & \dots \\ 0 & 0 & w_{4,3} & \dots \\ \vdots & \vdots & \vdots & \ddots \end{bmatrix} \tag{10}$$

is given in terms of the probabilities $w_{i,j} = \frac{1}{2}\min\Big(1, P_{\mathcal{J}}(q_i)/P_{\mathcal{J}}(q_j)\Big)$ $(i \neq j)$ to jump from state $q = q_j$ to $q = q_i = i/N$ in steps of $\Delta q = \pm 2$ or 0. Since T fulfills the detailed balance condition (with $P_{\mathcal{J}}$) it has only real eigenvalues. The largest eigenvalue (equal to one) is non-degenerate, and the second largest eigenvalue λ_1 determines the autocorrelation time of the chain (in units of sweeps),

$$\tau_B^q = -\frac{1}{N\ln\lambda_1} \approx \frac{1}{N(1-\lambda_1)} \; . \tag{11}$$

The associated effective free-energy barrier is finally defined as

$$F_B^q = \ln(\tau_B^q) \; , \tag{12}$$

which generalizes the standard formula $F_B^q = \ln[P_{\mathcal{J}}^{\rm max}/P_{\mathcal{J}}^{\rm min}] + {\rm const.}$ for the simple double-peak situation of first-order phase transitions.

For the analysis of the thus defined free-energy barriers we employed the peaked distribution function [22]

$$F_Q(x) = \begin{cases} F(x) \text{ for } F(x) \leq 0.5 \; ; \\ 1 - F(x) \text{ for } F(x) \geq 0.5 \; , \end{cases} \tag{13}$$

with $F(x)$ denoting the standard cumulative distribution function as given, e.g., in Ref. [13],

$$\frac{i}{n} - \frac{1}{2n} \leq F(x) \leq \frac{i}{n} + \frac{1}{2n} \quad \text{for} \quad x_i \leq x \leq x_{i+1} \ , \tag{14}$$

with straight-line interpolations in-between. For self-averaging data the function F_Q collapses in the infinite-volume limit to $F_Q(x) = 0.5$ for $x = [x]_{\rm av}$ and 0 otherwise. For non-self-averaging quantities the width of F_Q stays finite. The concept carries over to quantities which diverge in the infinite-volume limit, when for each lattice size scaled variables $x/x_{\rm med}$ are used.

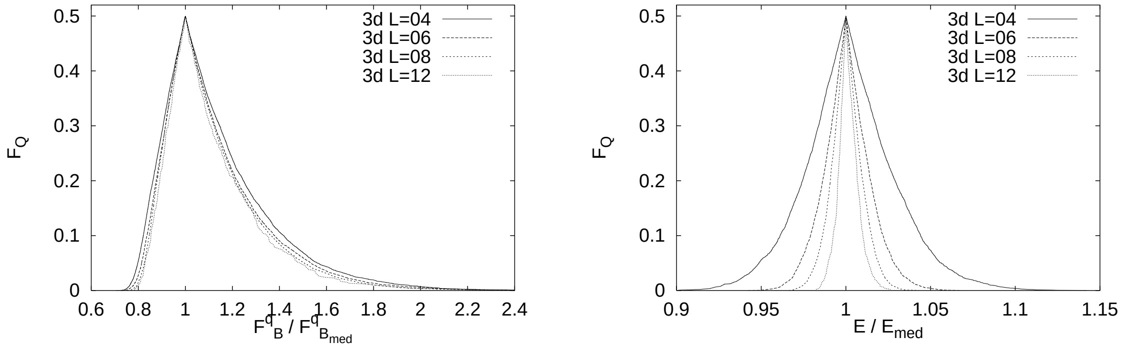

Figure 2: Distribution function F_Q as defined in Eq (13) for the $3d$ overlap barriers given in Eq (12) (left) and the energy (right) in units of their median values.

The behavior of $F_Q(F^q_B/F^q_{B_{\rm med}})$ shown on the l.h.s. of Figure 2 for the $3d$ case clearly suggests that F^q_B is a non-self-averaging quantity. In $4d$ the evidence is even stronger than in $3d$. Non-self-averaging was also observed for the autocorrelation times $\tau^{\rm muq}_{\mathcal{J}}$ of our algorithm while the energy is an example for a self-averaging quantity; cf. the r.h.s. of Figure 2. For non-self-averaging quantities one has to investigate many samples and should report the finite-size scaling (FSS) behavior for fixed values of the cumulative distribution function F. In Ref. [11] we performed for $F = i/16$, $i = 1, \ldots, 15$, fits to the ansatz

$$F^q_B = a_1 + a_2\, N^{1/3} \ , \tag{15}$$

corresponding to $\tau^q_B = e^{a_1}\, e^{a_2\, N^{1/3}}$, as suggested by investigations of barriers and autocorrelation times in the mean-field limit [23, 24]. In both dimensions the goodness-of-fit parameter Q [13] turned out to be unacceptably small. The $3d$ fits are depicted on the l.h.s. of Figure 3. We therefore tried fits to the ansatz

$$F^q_B = \ln(c) + \alpha\, \ln(N) \ , \tag{16}$$

corresponding to $\tau^q_B = c\, N^\alpha$; cf. the r.h.s. of Figure 3. Since in $3d$ as well as in $4d$ the average Q-value is now within the statistical expectation, the ansatz Eq (16) is strongly favored over Eq (15). As a function of F (= 1/16 – 15/16) the exponent $\alpha = \alpha(F)$ in the power law Eq (16) varies smoothly from 0.8 to 1.1 in $3d$ and from 0.8 to 1.3 in $4d$. A similar analysis for the autocorrelation times $\tau^{\rm muq}_{\mathcal{J}}$ of the multi-overlap algorithm gives exponents $\alpha(F)$ which are larger, $\alpha^{\rm muq}(F) \approx \alpha^q_B(F) + 1$. This re-iterates our previous observation that relevant barriers exist, which are invisible in the overlap variable q.

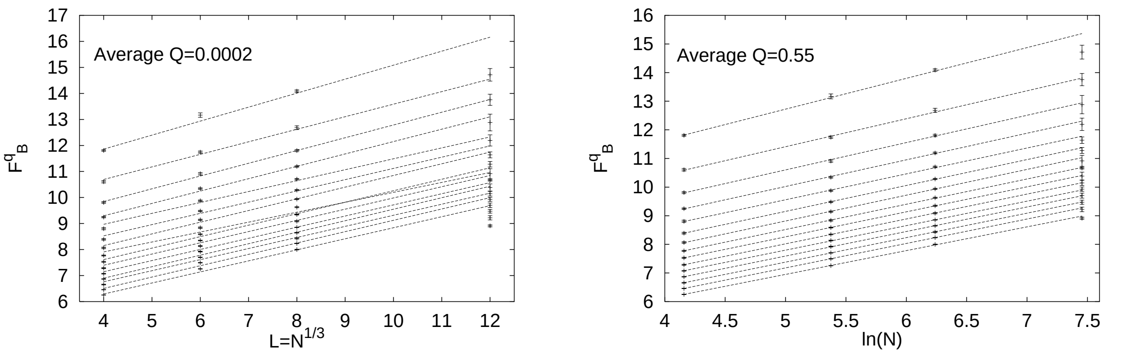

Figure 3: FSS fits at $F = i/16$, $i = 1, \ldots, 15$ (from down to up) of the $3d$ free-energy barriers F_B^q to the mean-field behavior in Eq (15) (left) and the logarithmic ansatz in Eq (16) (right).

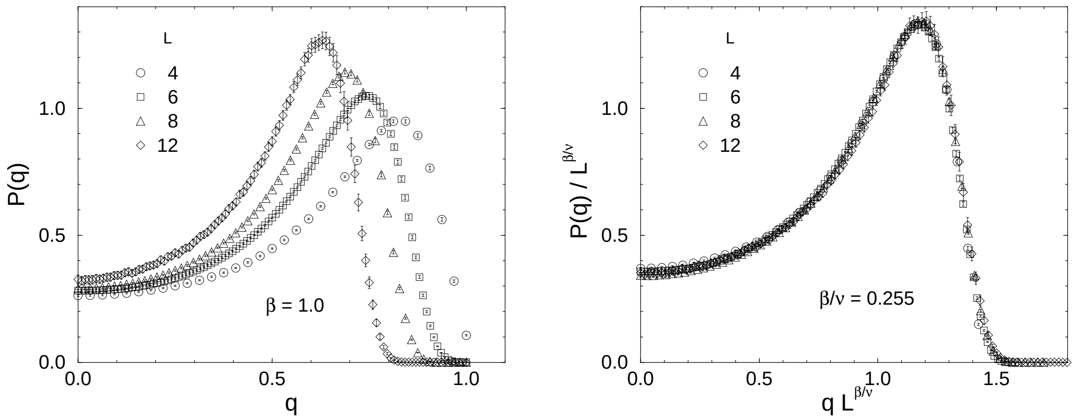

Figure 4: Averaged $3d$ probability densities $P(q)$ in raw (left) and scaled (right) form.

3.3 Finite-Size Scaling Behavior of Averaged Probability Densities

Let us start with the raw data for the averaged densities $P(q)$ which are shown on the l.h.s. of Figure 4 for the $3d$ model at the simulation point $\beta_0 = 1.0$. By applying reweighting techniques we estimated for the inverse freezing temperature $\beta_c \approx 0.88$ and found a FSS of the spin-glass susceptibility $\chi_{\rm SG} = N[\langle q^2 \rangle]_{\rm av} \propto L^{\gamma/\nu}$ with $\gamma/\nu = 2.37(4)$. Close to the transition point one expects that $P(q)$ satisfies the FSS relation $P(q) = L^{\beta/\nu}\hat{P}(L^{\beta/\nu}q)$. Using the scaling relation $\beta/\nu = (d - \gamma/\nu)/2 \approx 0.317$ this could indeed be confirmed at β_c [9]. More surprising is the fact that also in the spin-glass phase at the simulation point $\beta_0 = 1.0$ the data for different lattice sizes fall onto a common master curve when the value of β/ν is suitably chosen. This is demonstrated on the r.h.s. of Figure 4, where an exponent of $\beta/\nu = 0.255$ is used. This observation implies that the spin-glass phase is either governed by massless modes or that at least the correlation length ξ is large ($\xi > L_{\rm max} = 12$).

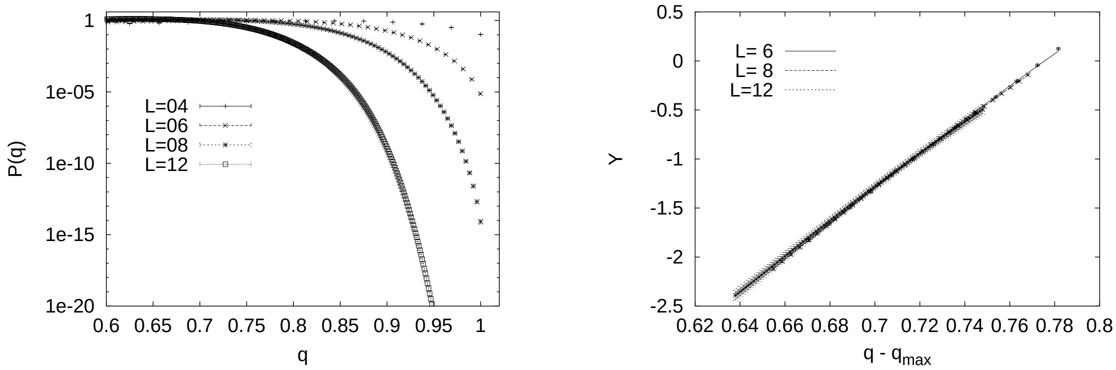

Figure 5: Tails of the $P(q)$ densities in $3d$ (left) and fits to the ansatz in Eq (18) (right).

3.4 Finite-Size Scaling Behavior of the Tails of $P(q)$

The multi-overlap algorithm becomes particularly powerful when studying the tails of the distributions which are highly suppressed compared to the peak values; see the l.h.s. of Figure 5 which depicts $P(q)$ over twenty orders of magnitude. Based on the replica mean-field approach, theoretical predictions for the scaling behavior of the tails have been derived by Parisi and collaborators [25]. They show that $P(q) = P_{\max}\, f(N\,(q - q_{\max}^{\infty})^x)$ for $q > q_{\max}^{\infty}$ and predict more quantitatively that

$$P(q) \sim \exp\left[-c_1\, N\,(q - q_{\max}^{\infty})^x\right] \quad \text{for} \quad N\,(q - q_{\max}^{\infty})^x \ \text{ large}, \tag{17}$$

with a mean-field exponent of $x = 3$. The additional condition $q \le q_{\mathrm{cut}} < 1$ ensures that q stays away from the lattice artefacts close to $q = 1$. By allowing for an overall normalization factor $c_0^{(N)}$ and taking the logarithm twice we have performed fits of the form [26]

$$Y \equiv \ln\left[-\ln(P/c_0^{(N)})\right] - \ln N = \ln c_1 + x\,\ln(q - q_{\max}^{\infty})\ . \tag{18}$$

To enforce the conditions $N\,(q - q_{\max}^{\infty})^x$ large as well as $q \le q_{\mathrm{cut}} < 1$ we restrict our fits to the q-range defined by $2^{-1}\,P_{\max} \ge P(q) \ge 2^{-10}\,P_{\max}$ which excluded the use of the $L = 4$ data in $3d$. The fits of the data from the remaining lattices in $3d$ are depicted on the r.h.s. of Figure 5. Leaving the exponent x as a free parameter, we arrived at the estimates

$$x = 12 \pm 2 \text{ in } 3d\ (\beta_0 = 1.0), \tag{19}$$

$$x = \ 5.3 \pm 0.3 \text{ in } 4d\ (\beta_0 = 0.6) \tag{20}$$

for the infinite-volume exponents which are much larger than the mean-field value of $x = 3$.

4 Summary and Conclusions

Employing non-Boltzmann sampling with the multi-overlap Monte Carlo algorithm we have investigated the probability densities $P_{\mathcal{J}}(q)$ of the Parisi order parameter q. The free-energy barriers F_B^q as defined in Eq (12) are found to be non-self-averaging. The logarithmic scaling ansatz Eq (16) for the barriers at fixed values F of their cumulative distribution function is favored over the mean-field ansatz Eq (15). Further, relevant barriers are still reflected in the autocorrelations of the multi-overlap algorithm.

The averaged densities exhibit a pronounced FSS collapse onto a common master curve even in the spin-glass phase. For the scaling of their tails towards $q = \pm 1$ we find qualitative agreement with the decay law predicted by mean-field theory, but with an exponent x that is, in particular in $3d$, much larger than theoretically expected.

Acknowledgements

W.J. would like to thank A. Aharony, K. Binder and E. Domany for useful discussions on non-self-averaging quantities.

References

[1] K.H. Fischer and J.A. Hertz, *Spin Glasses* (Cambridge University Press, Cambridge, England, 1991).

[2] A.P. Young (ed.), *Spin Glasses and Random Fields* (World Scientific, Singapore, 1997).

[3] M. Mézard, G. Parisi, and M.A. Virasoro, *Spin Glass Theory and Beyond* (World Scientific, Singapore, 1987).

[4] K. Binder and A.P. Young, *Rev. Mod. Phys.* **56**, 801(1986).

[5] G. Parisi, *Phys. Rev. Lett.*, **43**, 1754(1979).

[6] D.S. Fisher and D.A. Huse, *Phys. Rev.* **B38** 386(1988).

[7] C.A.M. Mulder, A.J. van Duyneveldt, and J.A. Mydosh, *Phys. Rev.* **B23**, 1384(1981); *Phys. Rev.* **B25**, 515(1982).

[8] P. Granberg, P. Svedlindh, P. Nordblad, L. Lundgren, and H.S. Chen, *Phys. Rev.* **B35**, 2075(1987), E. Vincent, J. Hammann, M. Ocio, J.-P. Bouchaud, and L.F. Cugliandolo, in: *Complex Behaviour of Glassy Systems*, ed. M. Rubi, Lecture Notes in Physics, Vol. 492 (Springer-Verlag, Berlin, 1997), pp. 184-219 [cond-mat/9607224], and references given therein.

[9] B.A. Berg and W. Janke, *Phys. Rev. Lett.* **80**, 4771(1998).

[10] W. Janke, B.A. Berg, and A. Billoire, *Ann. Phys. (Leipzig)* **7**, 544(1998); *Comput. Phys. Commun.* **121-122**, 176(1999).

[11] B.A. Berg, A. Billoire, and W. Janke, *Phys. Rev.* **B61**, 12143(2000).

[12] S.F. Edwards and P.W. Anderson, *J. Phys.* **F5**, 965(1975).

[13] W.H. Press, B.P. Flannery, S.A. Teukolsky, and W.T. Vetterling, *Numerical Recipes* (Cambridge University Press, Cambridge, England, 1986).

[14] B.A. Berg, *Fields Inst. Commun.* **26**, 1 (2000) [cond-mat/9909236].

[15] W. Janke, *Physica* **A254**, 164(1998).

[16] N. Kawashima and A.P. Young, *Phys. Rev.* **B53**, R484(1996).

[17] D. Badoni, J.C. Ciria, G. Parisi, F. Ritort, J. Pech, and J.J. Ruiz-Lorenzo, *Europhys. Lett.* **21**, 495(1993).

[18] G. Marsaglia, A. Zaman, and W.W. Tsang, *Stat. Prob. Lett.* **8**, 35(1990).

[19] M.L. Lüscher, *Comput. Phys. Commun.* **79**, 100(1994).

[20] B.A. Berg, U.E. Hansmann, and T. Celik, *Phys. Rev.* **B50**, 16444(1994).

[21] N. Metropolis, A.W. Rosenbluth, M.N. Rosenbluth, A.H. Teller, and E. Teller, *J. Chem. Phys.* **21**, 1087(1953).

[22] B.A. Berg, *Introduction to Monte Carlo Simulations and Their Statistical Analysis*, in preparation.

[23] N.D. Mackenzie and A.P. Young, *Phys. Rev. Lett.* **42**, 301(1982), *J. Phys.* **C16**, 5321 (1983). K. Nemoto, *J. Phys.* **A21**, L287(1988) G.J. Rodgers and M.A. Moore, *J. Phys.* **A22**, 1085 (1989). D. Vertechi and M.A. Virasoro, *J. Phys. (France)* **50**, 2325(1989).

[24] R.N. Bhatt, S.G.W. Colborne, M.A. Moore, and A.P. Young, unpublished, as quoted by Rodgers and Moore (Ref. [23]). See also S.G.W. Colborne, *J. Phys.* **A23**, 4013(1990). H. Kinzelbach and H. Horner, *Z. Phys* **B84**, 95(1991). A. Billoire and E. Marinari, Preprint cond-mat/0101177.

[25] S. Franz, G. Parisi, and M.A. Virasoro, *J. Phys. I (France)* **2**, 1869(1992). G. Parisi, F. Ritort, and F. Slanina, *J. Phys.* **A26**, 3775(1993). J.C. Ciria, G. Parisi, and F. Ritort, *J. Phys.* **A26**, 6731(1993).

[26] B.A. Berg, A. Billoire, and W. Janke, Preprint in preparation.